

Tidal stream resource assessment through optimisation of array design with quantification of uncertainty

D. M. Culley^{*†}, S. W. Funke[‡], S. C. Kramer[†], M. D. Piggott[†]

[†] Applied Modelling and Computation Group, Department of Earth Science and Engineering,
Imperial College London, London, SW7 2AZ, UK

[‡] Center for Biomedical Computing, Simula Research Laboratory, Oslo, Norway

* Corresponding author: dmc13@imperial.ac.uk

Abstract—As the number of tidal stream turbines within an array increases, so the effects of that array on the flow and environment accumulate. Many key objective measures (such as energy yield or financial profit) begin to suffer the effects of diminishing increases. Optimising the layout of individual turbines within an array – micro-siting – facilitates significantly increased energy harvest for a given number of turbines in a given area, as compared to a ‘human’s best attempt’ design. The optimal micro-siting design of an array, and therefore an accurate forecast of the yield of that array, must be found as the product of an optimisation exercise which may incorporate turbine parameters, local bathymetry and a host of other practical, physical, legal, financial or environmental constraints.

The number of turbines within an array proposed for a given site has an even greater effect on the yield of that array. Determining the optimum number of turbines is, therefore, a problem of critical importance. Like the micro-siting design, this also cannot be solved directly but must be approached through a process of iterative optimisation. Consequently, only through determining the optimal number of turbines and their arrangement, can a reliable estimate of the accessible tidal resource on a site be made. Making this determination is, however, computationally intensive. In this paper, tools from statistical decision theory, such as surrogate modelling and variable fidelity sampling, are used to efficiently allocate computational effort where it provides most value in the optimisation of the number of turbines. This enables the array design problem to be tackled much more efficiently than would be possible using more conventional optimisation approaches. Finally, having determined the optimal array design it is imperative that the sensitivity of the design to modelling assumptions can be quantified and fully understood.

This paper focuses on a brief exploration of three aspects of resource assessment through array design: Firstly, *TidalArraySizer* is presented, this is a framework for the optimisation of tidal turbine array size built upon *OpenTidalFarm* project. Secondly developments are presented which provide *OpenTidalFarm* with functionality to measure the sensitivity of the objective function with respect to the modelling parameters. Thirdly, these contributions are demonstrated on an example based upon the Inner Sound of the Pentland Firth.

Index Terms—Tidal array optimisation, tidal stream resource assessment, uncertainty quantification, array micro-siting, array sizing.

I. INTRODUCTION

Tidal stream turbines generate power from tidally induced currents by converting water momentum into electricity. To

extract energy on an industrial scale, an array consisting of multiple devices, typically 10’s to 100’s, needs to be installed on a tidal site with highly energetic flow regimes. The additional resistance from the turbines impacts upon the flow, both in the near-field as well as potentially in the far-field, and results in a coupled hydrodynamic system in which flow velocities vary greatly on a wide range of spatial scales. Furthermore, the turbine’s power production is approximately proportional to the cube of the velocity at the turbine location, and is hence strongly sensitive to flow changes. Thus determining how many turbines to place in a given region of interest, and their location within the site is a complex, coupled problem, but critical for estimating the extractable resource at that region.

In fact, [1]–[4] demonstrated that the extractable power from an array is heavily contingent upon the location of the turbines (also called the ‘micro-siting’ design), demonstrating improvements in the power extracted from the flow of up to 40% as compared to a regular grid layout. Since the design problem is strongly coupled to spatially varying and time dependant hydrodynamics, it is challenging to determine by intuition what the optimum turbine layout for a given number of turbines on a given site may be. Instead, the micro-siting design must be optimised through a process of iterative improvement, a framework for which is laid out in [1]. This means that the power that may be extracted by a certain number of turbines cannot be accurately diagnosed without having determined their optimum layout.

Additionally, the highly coupled nature of the problem means that the optimal number of turbines to place on a site can also not be determined *a priori*. The additional problem here, is that diagnosing the potential power output of a given number of turbines on the region requires the location of those turbines to first be optimised. So in optimising for the number of turbines, we have a nested ‘inner’ micro-siting optimisation every time we wish to make an evaluation for the number of turbines. With realistically sized problems this can easily become computationally intractable. Therefore, the problem is to allocate the available computational budget in a manner that will provide a reliable assessment of the potential resource at

a given site within a reasonable time.

Finally, it is imperative that some accounting is made of the risk and uncertainty attached to the estimate of available resource that is made. Understanding the sensitivity of a given solution with respect to the input parameters goes some way to providing developers with an understanding as to which information is most important to survey and feed into the next phase of more detailed site investigation.

In this paper, a framework for resource assessment is presented which integrates cost modelling, sensitivity analysis and realistic array design in order to produce a practical tool for evaluating potential tidal stream power development sites. In the following sections, the micro-siting design problem is defined, and *OpenTidalFarm* introduced as a framework for tackling it. Next, a surrogate modelling framework, *TidalArraySizer*, is discussed which, working in concert with *OpenTidalFarm*, enables optimisation of the array size. The novel contribution of this work is development of *OpenTidalFarm* to provide sensitivity data, and the creation of *TidalArraySizer*. The interested reader is directed toward [1], [3], [5] for more information on the *OpenTidalFarm* project. Having found the optimal number of turbines and their micro-siting design, the process of sensitivity analysis is discussed in section V. This process is then applied to a highly idealised test scenario based upon the Inner Sound of the Pentland Firth.

II. PROBLEM DEFINITION

Increasing the turbine number on a tidal site first increases the farm's power production up to the point where the additional blockage begins to significantly deflect flow around and away from the turbine site. This results in a reduction of the power extracted per turbine, and eventually a decrease in the total farm production as more and more turbines are introduced into the array [6], [7]. Therefore, the return on investment per turbine diminishes with increasing number of turbines. Since tidal turbines have very high capital costs, it is important that a resource assessment takes this cost into account, in relation to the extractable resource. For example, one could imagine that the farm that is financially viable on a given site extracts just a fraction of the theoretically available resource.

Hence, rather than maximising power extraction on a given site, we instead optimise the array size and micro-siting design to maximise the financial return for the developer. That is, our goal is to find the number of turbines n in the farm and their position $\vec{m} = (x_1, y_1, x_2, y_2, \dots, x_n, y_n)^T$ such that the financial return

$$R_{\text{fin}}(n, \vec{m}) = I(P(\vec{m})) - C(n) \quad (1)$$

is maximised. Here, $P : \mathbb{R}^{2n} \rightarrow \mathbb{R}$ evaluates the farm's total energy extraction throughout its lifetime and $I : \mathbb{R} \rightarrow \mathbb{R}$ converts this energy into income. $C : \mathbb{R} \rightarrow \mathbb{R}$ denotes the cost of the farm, where, for simplicity, we assume that the cost only depends on the number of turbines and not their location within the farm. The inclusion of location-specific cost terms in the micro-siting design process has been discussed in [5].

The farm's power extraction from the flow is computed from

$$P(\vec{m}) = \frac{1}{T} \int_0^T \int_{\Omega} \rho c_t(\vec{m}) \|\vec{u}(\vec{m})\|^3 dx dt, \quad (2)$$

where Ω is the computational domain, $(0, T)$ is the simulation period, ρ is the density of water and c_t is a parametrisation of the turbine farm via a friction field only present at the locations of individual turbines (see [1] for more details). The depth-averaged flow velocity, $\vec{u} : \Omega \times [0, T] \rightarrow \mathbb{R}^2$ is the solution to the non-linear shallow water equations

$$\begin{aligned} \frac{\partial \vec{u}}{\partial t} + \vec{u} \cdot \nabla \vec{u} - \nu \nabla^2 \vec{u} + g \nabla h + \frac{c_b + c_t(\vec{m})}{H + h} \|\vec{u}\| \vec{u} &= 0, \\ \frac{\partial h}{\partial t} + \nabla \cdot ((H + h) \vec{u}) &= 0, \end{aligned} \quad (3)$$

where $h : \Omega \times [0, T] \rightarrow \mathbb{R}$ is the free surface perturbation, $H : \Omega \rightarrow \mathbb{R}$ is the water depth at rest, ν is the viscosity coefficient, and c_b and c_t are the natural bottom and the farm induced bottom friction respectively.

For a fixed number of turbines, n , the maximum revenue is computed by solving the *continuous* optimisation problem

$$\begin{aligned} \tilde{R}_{\text{fin}}(n) &= \max_{\vec{m} \in \mathbb{R}^{2n}} I(P(\vec{m})) - C(n) \\ \text{subject to } b_l &\leq \vec{m} \leq b_u \\ g(\vec{m}) &\leq 0. \end{aligned} \quad (4)$$

The first optimisation constraint prevents turbines from leaving the leased turbine area. If the leased turbine area is rectangular then this may be represented as in (4) where b_l and b_u represent the lower and upper boundaries respectively. However, more general area constraints could be incorporated. The inequality constraint $g(\vec{m}) \leq 0$ prevents turbines being situated too closely to one another.

where b_l and b_u represent the lower and upper boundaries of the turbine area respectively (we assume a rectangular farm area for simplicity), and the inequality constraint $g(\vec{m}) \leq 0$ is chosen such that it enforces a minimum distance between each turbine.

The number of turbines resides in the integer space, so the optimum number of turbines is found via the *integer* optimisation problem

$$\hat{R}_{\text{fin}} = \max_{n \in \mathbb{N}} \tilde{R}_{\text{fin}}(n) \quad 0 \leq n \leq n_{\text{max}}, \quad (5)$$

where n_{max} is an upper constraint on the number of turbines that the site is capable of supporting, which can be calculated from the minimum turbine distance constraints and the turbine lease area or the number of turbines the developer can afford.

III. OPENTIDALFARM

OpenTidalFarm is an open source software project for solving the optimisation problem (4). It is built upon the finite element framework *FEniCS* [8] and relies on gradient-based optimisation methods to efficiently optimise even large farms with hundreds of turbines. In each optimisation iteration,

OpenTidalFarm predicts the performance of the farm design by solving the shallow water equations (3) using the Taylor-Hood element pair [9] and evaluating (1). It then computes the gradient $dR_{\text{fin}}/d\vec{m}$ using the adjoint approach with the *dolfin-adjoint* library [10], [11]. The optimisation method then uses this information to update the turbine locations, \vec{m} , to increase R_{fin} until the convergence criteria have been met.

The adjoint approach provides computationally economical access to the derivative of the farm revenue with respect to the turbine positions at a fraction of the cost of one shallow water solve. In particular this gradient computation is practically independent of the number of turbines. Access to gradient information is the key to gradient-based optimisation methods which can be orders of magnitude more efficient than derivative-free optimisation methods such as genetic algorithms (e.g. taking $\mathcal{O}(10^2)$ evaluations as opposed to $\mathcal{O}(10^5)$ or more evaluations) [3]. Since fewer evaluations are required, the available computational budget can be allocated to increase the fidelity of the hydrodynamic model. This is what enables a full, coupled solve of (3) and (4), and hence a more realistic representation of the flow and evaluation of the power to be performed at each evaluation iteration.

IV. TIDALARRAYSIZER

Optimising the array size through sampling different values of n requires *OpenTidalFarm* to be run multiple times. This can easily become computationally exorbitant if done naively. If we treat *OpenTidalFarm* as an unknown, non-linear solver taking as input n and returning \tilde{R}_{fin} (and supplementarily \vec{m}) then there are various techniques (especially from aerospace design research [12]) to efficiently optimise expensive functions.

Treating *OpenTidalFarm* in this way, as a ‘simulation’ model whose fidelity we may control through adjustment of the convergence criteria, facilitates use of an approximation or ‘surrogate’ model framework. Gaussian process regression has been chosen for this application because it can support variable-fidelity simulation sampling and faithfully accounts for uncertainty in the regression. The particular surrogate model framework developed for application to this problem will be referred to as *TidalArraySizer* to distinguish design choices specific to this model from surrogate models in general.

A. Gaussian Process Regression

Consider a bivariate Gaussian representing the probability density function (pdf) of a function evaluated at two points (figure 1). By parametrising the mean and covariance of that pdf, we control our expectations of the relationship between the function evaluated at the two points. If an observation of the function is then made at one of those points (shown on the graph as a thick black line), the Gaussian distribution enables us to calculate (in closed form) the conditional pdf for the other point. I.e. we are able to use rigorous learning theory to estimate the value of the function at one point using the function observed at another point (the red line in figure 1).

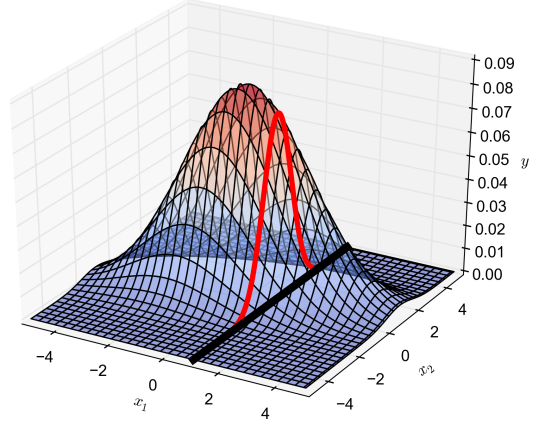


Fig. 1. Linking two points using a bivariate Gaussian distribution enables the conditional pdf (red) for the function at the unknown point x_2 to be calculated based upon the known point x_1 .

This process can be generalised to a multivariate Gaussian representing multiple points, and hence we can determine the conditional pdf of the function evaluation at any of those points based on observations at one or more of the other points. In the same way that the bivariate Gaussian was described by a mean and covariance, so too is the multivariate Gaussian parametrised by a mean function and a kernel function which provide the user with the opportunity to encode prior assumptions about the behaviour of the underlying function. For example, in *TidalArraySizer* we choose a squared exponential kernel function

$$\kappa(x, x') = \sigma_f^2 \exp\left(-\frac{1}{2l^2}(x - x')^2\right), \quad (6)$$

as the covariance function where x and x' are two inputs. This represents the assumption that similar inputs will produce similar outputs – the similarity of which may be estimated by the exponential of the squared difference of the inputs. The ‘hyper-parameters’, l and σ_f^2 represent the (horizontal) length scale and maximum allowable covariance (i.e. related with vertical axis scale) respectively and allow the function to be ‘tuned’ to the particular problem. This tuning may be done in different ways, in *TidalArraySizer* the hyper-parameters are optimised through maximising the marginal likelihood, explanation of this is beyond the scope of this paper, but is outlined in [13] and [14].

Full discussion of Gaussian processes is beyond the scope of this paper, however, for the purposes of this work, one of the key benefits of this framework is that it reflects the uncertainty inherent to our estimate of the function away from sampled points. Furthermore, points can be added with ‘error’ bars. This enables samples of varying fidelity to be used, as the lower reliability of a scaled low-fidelity sample can be incorporated, allowing it to be used within the same regression framework as a non-scaled high fidelity sample. Fidelity control, sample selection and scaling are parts of what is termed the ‘design of experiment’.

B. Design of Experiment

The structure of our chosen surrogate model means that while we have confidence in accurately estimating the underlying function close to sampled points, the model does not generalise well in areas where observations have not been made. As such, the choice of how many points to sample, and where those samples should be taken is critical – especially because the computational cost of the process of optimising n is directly proportional to the number of samples taken.

Fortunately, since we are looking to find the optimum number of turbines, we do not require *TidalArraySizer* to generalise well – i.e. represent a good input / output mapping across the complete range of $0 \leq n \leq n_{\max}$. Instead, we wish to be sufficiently sure of the trend over the whole range of n that we have identified the region containing the global optimum, and then produce an accurate mapping of that region. This is where variable fidelity sampling and scaling becomes particularly useful. In this case, the fidelity is varied by adjusting the convergence criteria on the *OpenTidalFarm* optimisation – with looser criteria (and hence lower inner iteration counts) corresponding to a lower fidelity run.

1) *Variable Fidelity Sampling and Scaling*: Samples taken at a lower fidelity can be scaled so that they can be used in combination with higher fidelity samples in constructing the surrogate model. Since sensitivity information with respect to n is unavailable, *TidalArraySizer* is limited to using a multipoint correction based on additive and multiplicative zeroth order scaling [15]. What this means is that if $P_{\text{lo}}(n)$ is the power found with loose convergence criteria and $P_{\text{hi}}(n)$ is the same but with more stringent convergence criteria (i.e. higher fidelity), then the multiplicative and additive scaling factors respectively are defined as

$$A(n) = \frac{P_{\text{hi}}(n)}{P_{\text{lo}}(n)}, \quad (7)$$

$$B(n) = P_{\text{hi}}(n) - P_{\text{lo}}(n). \quad (8)$$

Then the multipoint corrected scaled low fidelity model at n based on two other design points n^0 and n^1 is

$$P^*(n) = \gamma(P_{\text{lo}}(n) + B(n^0)) + (1 - \gamma)A(n^0)P_{\text{lo}}(n), \quad (9)$$

where

$$\gamma = \frac{P_{\text{hi}}(n^1) - A(n^0)P_{\text{lo}}(n^1)}{P_{\text{lo}}(n^1) + B(n^0) - A(n^0)P_{\text{lo}}(n^1)}. \quad (10)$$

2) *Design of Experiment*: The user of *TidalArraySizer* selects two sets of convergence criteria for *OpenTidalFarm*, this defines the low and high fidelity model. Both low and high fidelity results can be obtained in one optimisation run with no additional overhead, as the high fidelity is simply a continuation of the low fidelity run.

The group of design points at which P has been evaluated are called the training set, \mathcal{D} , based upon which the

surrogate model is constructed. Upon initialising the experiment, *OpenTidalFarm* is run at low fidelity (i.e. with looser convergence criteria) for n_{\max} and $n_{\max}/2$, and the surrogate model is constructed based on the training set of three points, $\mathcal{D} = \{P(0), P(n_{\max}/2), P(n_{\max})\}$ where $P(0) = 0$ of course. The surrogate model provides the expected values of P , $\mathbb{E}(P)$, at all $0 \leq n \leq n_{\max}$ and the 95 % confidence interval is also calculated as 1.96 standard deviations from the mean (since we are using a Gaussian distribution).

The next low fidelity sample is taken at $\text{argmax}_n(\mathbb{E}(P) + 1.96\sigma)$. Low fidelity samples continue to be taken until n_{opt} has been identified to within ± 20 turbines. The algorithm then switches to high fidelity and tests samples at $\text{argmax}_n(\mathbb{E}(P))$. Once two high fidelity samples have been taken, the low fidelity points are scaled as detailed in section IV-B1 – though the scaled points are passed to the surrogate with error bars equal to the amount they have been scaled.

TidalArraySizer can keep sampling until the optimum has been found to the nearest n , however this level of accuracy may not be realistic given the simplifying assumptions made in setting up the hydrodynamic problem – for large-scale simulations operating on a desktop size machine parameters such as mesh resolution and viscosity may be chosen to provide a sufficiently simplified problem – in these conditions, a tolerance of circa 5 has been observed to be more suitable.

V. SENSITIVITY ANALYSIS

Another benefit of the *OpenTidalFarm* framework is the accessibility of sensitivity (i.e. gradient) information thanks to its adjoint model. Not only is the sensitivity of the power with respect to the turbine locations available (used to optimise the micro-siting design as has been discussed), but also with respect to any other physical input parameter. In particular, the three parameters of interest from the shallow water equations (3) are the bathymetry – parametrised through H , the natural bottom friction, c_b and the viscosity coefficient, ν .

In [16] the sensitivity with respect to bottom friction of the power generated by a turbine deployment in the Pentland Firth was explored by respectively doubling and halving the uniform coefficient that had been applied over the whole domain, and studying the effects. In the *OpenTidalFarm* framework, once the optimal array size and micro-siting design has been found, the spatial sensitivity to model parameters (such as bottom friction) can be computed using the adjoint approach. Thus rather than having a snapshot of how the amount of power extracted may vary as the bottom friction is changed uniformly over the whole domain, as in [16], *OpenTidalFarm* provides more complete information as to the areas in the domain where the modelling assumptions that have been made may impact most upon the power extracted by the array. From a resource assessment standpoint this is very useful as it highlights areas within the domain that require special attention during the next phase of more detailed numerical modelling or potentially physical site surveying.

TABLE I
PARAMETER VALUES USED FOR ORKNEY CASE-STUDY

| Parameter | Symbol | Units | Value |
|------------------------------|--------|----------------------------|--------|
| Water depth | H | m | 50 |
| Viscosity coefficient | ν | $\text{m}^2 \text{s}^{-1}$ | 30 |
| Acceleration due to gravity | g | m s^{-2} | 9.8 |
| Water density | ρ | kg m^{-3} | 1000 |
| Turbine friction coefficient | K | | 12 |
| Bottom friction coefficient | c_b | | 0.0025 |
| Turbine radii | r | m | 10 |

VI. CASE STUDY

To demonstrate the utility of the *TidalArraySizer* framework, the array design was optimised for an idealisation of a real-world tidal array site in the Inner Sound of the Pentland Firth. This site is currently under development by MeyGen Ltd (meygen.com) whose proposal sees the site developed in two phases. In phase 1, 86 MW of capacity will be installed in the area shown in figure 2.

A. Problem Set-Up

For this work, the model has been simplified to make the problem tractable for a desktop computer (8 cores) to tackle in circa 1 week. The *TidalArraySizer* code is very lightweight and therefore the computational expense of an optimisation is driven by *OpenTidalFarm* for which [1] demonstrated scalability on 64 cores. With a greater computational resource, the physics of the problem can be represented more accurately than is achieved in this case study. Assumptions such as a coarse mesh size, high viscosity, close-in domain boundaries and flat bathymetry are made here to keep the problem manageable in size. The problem is currently being rerun using HPC with a more realistic representation of the physics by making more realistic parameter assumptions than are made here. The results of this will be reported in future publications.

The computational domain, with overlaid mesh is shown in figure 3 where the red line shows the turbine area. Inside the turbine area the mesh resolution is 2 m, while away from the area – for example at the north of the island, the resolution decreases to 750 m. The bathymetry is assumed constant at $H = 50$ m. Running a time dependent problem on such a large domain is pushing the capabilities of a desktop machine – hence the number of degrees of freedom to the north of the island is severely limited. Perhaps more crucially the extent of the domain is also very limited. The boundary conditions prescribe the inflow velocity by a Dirichlet condition enforcing a sinusoidal velocity profile over 12 hours, fluctuating from $\pm 2 \text{ ms}^{-1}$. The timestep was set to 12/9 hours. The viscosity was set to $30 \text{ m}^2 \text{s}^{-1}$ to ensure the stability on the mesh used – however in future work, use of HPC resources will enable the optimisation to be run at much higher spatial and temporal resolution and the viscosity coefficient may then be reduced accordingly.

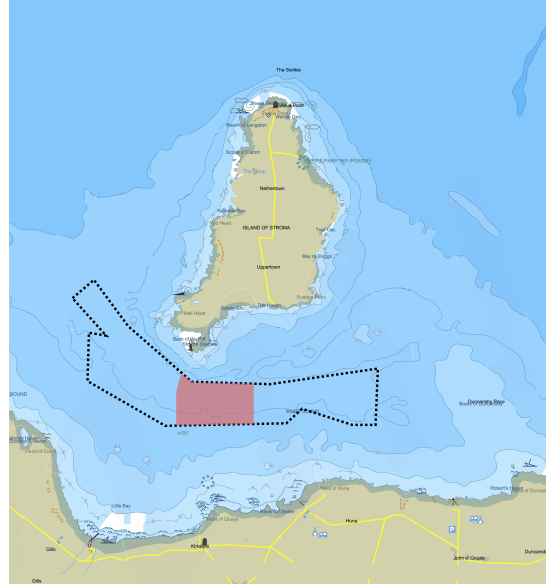


Fig. 2. Map of the Inner Sound of the Pentland Firth showing the site for phase 1 of the tidal turbine array development project by Meygen (meygen.com). The shaded red shows the phase 1 deployment area, on which the turbine area for testing is based (see figure 3).

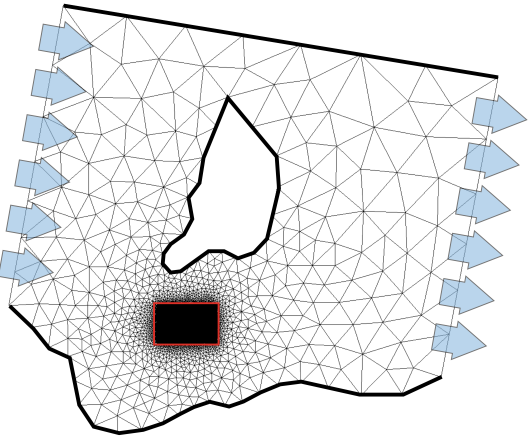


Fig. 3. Mesh for the case study based on the Inner Sound of the Pentland Firth, mesh size varies from 2 m in the turbine area (denoted by the red box) to 750 m.

The boundaries to the north and south of the domain, as well as for the island itself are modelled as free-slip. The mesh resolution and narrowness of the channel to the north of the island will cause an artificial increase in the resistance to the flow in this region. For this work, the case-study is being used as a proof of concept – to demonstrate this approach, however for a more realistic run, this northern boundary will be moved outward to improve the hydrodynamic representation of the real-world problem.

Recall from (1) that we also require functions $I(P)$ and $C(n)$. Such information is commercially sensitive and therefore unavailable for academic publication. For the purposes of this work, a cost of £3m per turbine and income of £4.7m

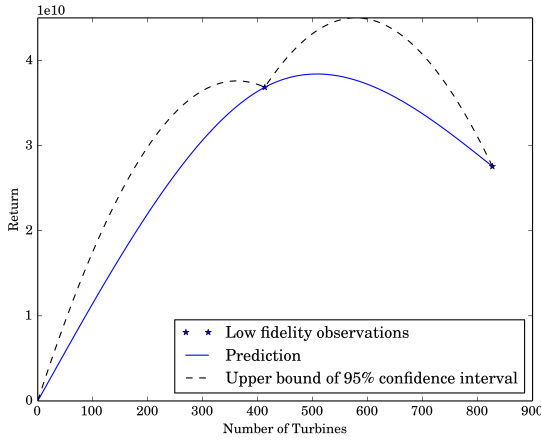


Fig. 4. Plot showing the Gaussian process regression performed on the initialised dataset. The dotted line shows upper bound of the 95 % confidence interval (as we are attempting to maximise power, we are not interested in the lower bound).

per MW of installed capacity has been assumed. Clearly the optimum number of turbines returned by the model will be sensitive to these assumptions. An increase in income per MW will likely result in the optimum number of turbines being increased, while an increase in the cost per turbine will reduce the optimum number that should be installed on a site.

The stopping criteria at the i th iteration is defined by $|P^{i-1} - P^i| < \alpha P^0$. For P_{lo} , $\alpha = 0.25$ for P_{hi} , $\alpha = 0.01$.

B. Optimisation

1) *Initialisation:* The run was initialised with low fidelity samples at $n_{\max} = 827$ and $n_{\max}/2 = 413$ turbines. Along with $P(0) = 0$ this provides the initial training set for construction of the surrogate, shown in figure 4. Here we see that $\max(\mathbb{E}(P) + 1.96\sigma)$ is located in the upper unexplored interval at $n = 556$ testing this point indicates that the optimum is located in the interval $0 < n < 413$ and the maximum upper bound of the confidence interval occurs at $n = 298$ so this point is tested. This process continues until the prediction (shown by a solid blue line on the plots) indicates that the optimum is within the tolerance of ± 20 . This occurred within 7 low fidelity samples, the complete set of low fidelity points are plotted in figure 5.

2) *High Fidelity Testing:* Now that the trend over the complete range has been explored at low fidelity, the algorithm begins to close in towards the optimal n using high fidelity runs. The first high fidelity run is taken at $n = 91$, this gives an improvement of 27 % as compared to the low fidelity sample at this location. The next sample is taken at $n = 68$, giving an improvement of 30 % as compared to the low fidelity sample at this location. This gives the basis for multipoint correction of the low fidelity samples. These high fidelity samples and the scaled low fidelity points are plotted in figure 6. Note that error bars on the scaled samples grow away from the points at which the multipoint correction was calculated and also that the uncertainty no longer ‘pinches’ in fully at these points as

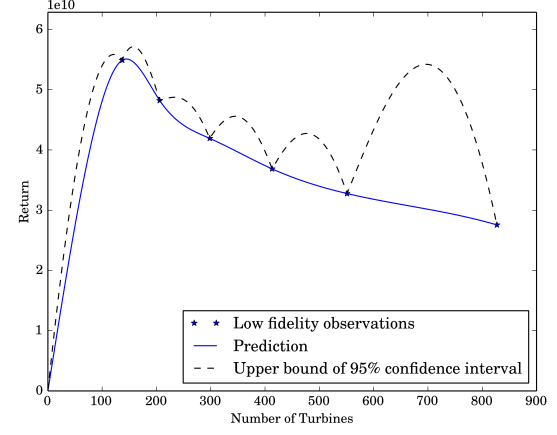


Fig. 5. Plot showing the complete set of low fidelity samples before high fidelity testing begins. While the uncertainty is peaking at $n = 720$ we are sufficiently confident in having identified the trend that points are sampled based on the maximum of the prediction rather than the maximum of the uncertainty.

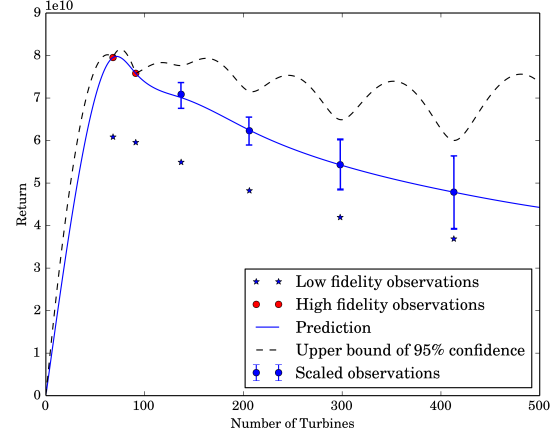


Fig. 6. With two high fidelity samples, the low fidelity samples can be scaled. Error bars reflect the uncertainty that is introduced through this sampling.

there is more uncertainty attached to these observations than there is for the sampled high fidelity points.

The optimisation continues making observations at high fidelity until the optimum has been identified to within ± 5 turbines. The final plot showing the optimum at $n = 80$ is shown in figure 7.

This optimised array produces 2.15 times the power of the fully populated, $n = 827$, array. This is because the overall blockage of the flow by the array has been appropriately balanced against the power generated by adding turbines. If, rather than optimising for financial return, the goal was to maximise power, this experiment indicates an array size of circa 95 turbines would be optimal.

On this example, the benefit of using variable fidelity sampling was significant. Optimising a time dependent problem is computationally expensive and the high fidelity runs in this example took circa 8 times the amount of time to compute (on three cores a low fidelity run took approximately half a day, while a high fidelity run took 3-4 days). While the multi-

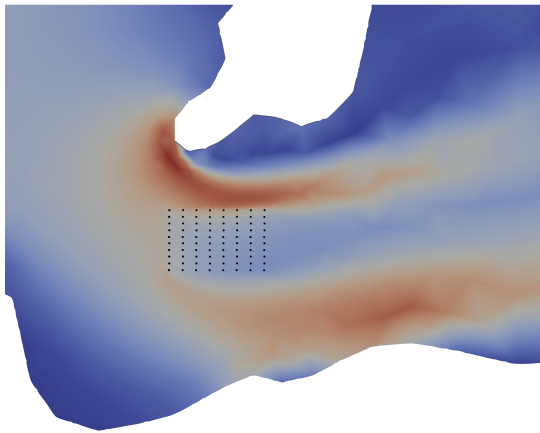


Fig. 7. The starting array micro-siting design for *OpenTidalFarm* is a regular grid. The plot shows velocity magnitude during peak flood. (Flow from left to right across the domain).

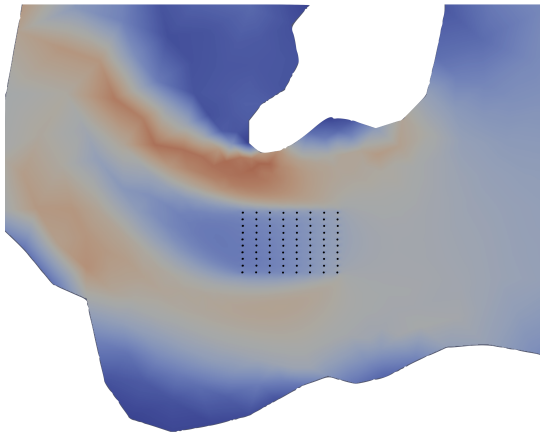


Fig. 8. Starting array configuration showing velocity magnitude during peak ebb. (Flow from right to left across domain).

fidelity sampling adds some complexity to the methodology, it does result in significant savings in computation.

3) *Results:* It is instructive to look at the array layout for the optimum array size overlaid with the magnitude of the flow velocity as in figures 8, 9, 10 and 11. Each *OpenTidalFarm* optimisation begins with the turbines arranged in a regular grid layout, the effect of this array on the flow for the maximum flood and ebb velocities respectively are shown in figures 8 and 9 in the case of $n = 80$. This may be compared to the effect of the optimised array micro-siting design which can be seen in figures 10 and 11, again for the flood and ebb phases respectively.

The optimum array micro-siting design shows clear barrage-like structures arranged perpendicular to the jet coming off the south of the island during the flood phase. The geography of the island means that a weaker jet develops off the other side of the island during the ebb phase, consequently there is less available power flowing through the site and as such these turbine barrages are less well orientated to extract energy when the flow is in this direction and the arrangement seems

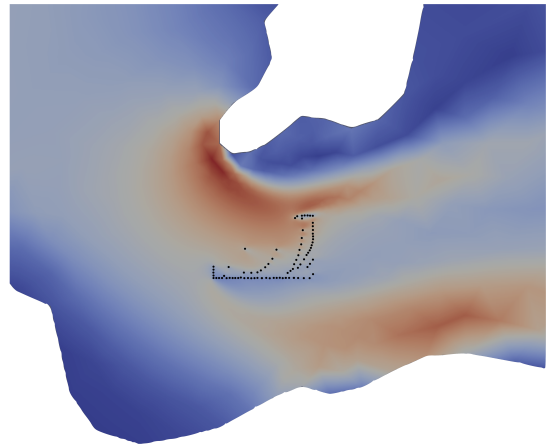


Fig. 9. Optimised array micro-siting design during peak flood.

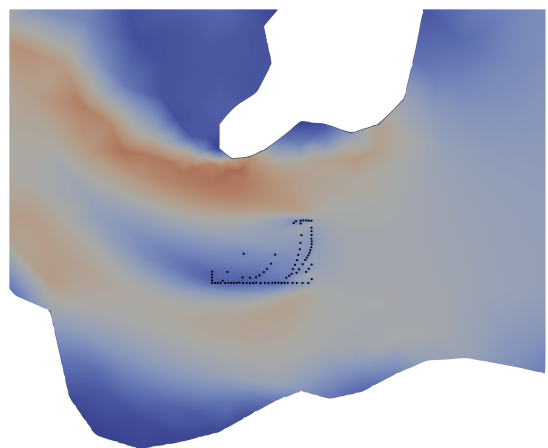


Fig. 10. Optimised array micro-siting design during peak ebb.

to be flood-dominant in design.

One major reason for this is that the turbines are not parametrised with power or thrust coefficients which vary with velocity. Such parametrisation would enable the maximum energy extracted to be capped at the design velocity. This capping would reduce the ratio between power extracted in the flood versus ebb phase and thus reduce the flood dominance of the design. More accurate turbine parametrisation is a primary focus for future work by the author.

From the initial configuration in figures 8 and 9 to the optimised design in figures 10 and 11 is an improvement of power extracted over the 12 hour period of 24 % which is obviously very significant. This is especially the case when considered in terms of financial return (as shown in figure 7) where a difference of just a few percent could make the difference between a scheme that is viable and one that is not.

C. Sensitivity Analysis

Having determined the optimum number of turbines and their micro-siting design, we can run a sensitivity analysis to determine the impact that some of the parameter choices had upon the solution. Figures 12, 13 and 14 are plots showing

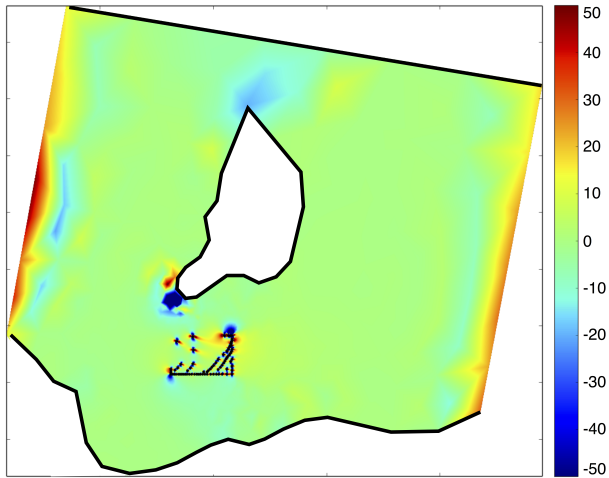


Fig. 11. Plot showing sensitivity of the power extracted from the flow with respect to the depth. The colour bar shows dP/dH .

the sensitivity of the power extracted from the flow with respect to the depth, bottom friction and viscosity coefficient respectively.

1) *Depth*: Figure 12 shows the sensitivity of the power to the assumption of a uniform depth of 50 m across the domain. Clearly there are some boundary effects at the inflow / outflow of the domain, given greater computational resource it would be desireable to move these boundaries much further away from the area of interest. As would be expected, power is sensitive to depth at the north of the island (shallower depth here would force flow south of the island and increase energy flux through the turbine area) and immediately south of the island (again, shallower bathymetry would skew the flood-time jet more into the turbine area). There are also some smaller scale sensitivity fluctuations immediately around the turbines – changes in depth here would help funnel flow into the turbine; acting somewhat akin to ducting. This effect would, however, need to be modelled at much higher resolution (and likely in three-dimensions) to be explored fully.

2) *Friction*: Figure 13 shows the sensitivity of the power with respect to the bottom friction, c_b . Here again the dominance of the flood-tide jet off the south of the island to the configuration of the array and the power it extracts is clearly visible. Reduced bottom friction to the south of the island would draw the jet into the turbine area. Similarly if the friction to the north of the island were greater than assumed for this run, then flow would be redirected to going South of the island, again increasing flow through the turbine area.

3) *Viscosity*: Arguably the least realistic assumption in the experiment here is the high viscosity coefficient which is required for numerical stability. Figure 14 shows the impact of that assumption is predominantly localised around the array. To the south of the turbine area where the turbines have lined up along the turbine area boundary the plot shows the power has high sensitivity with respect to viscosity. This is due to the boundary layer forming in the flow around the array. With lower viscosity this would be much less well defined, and

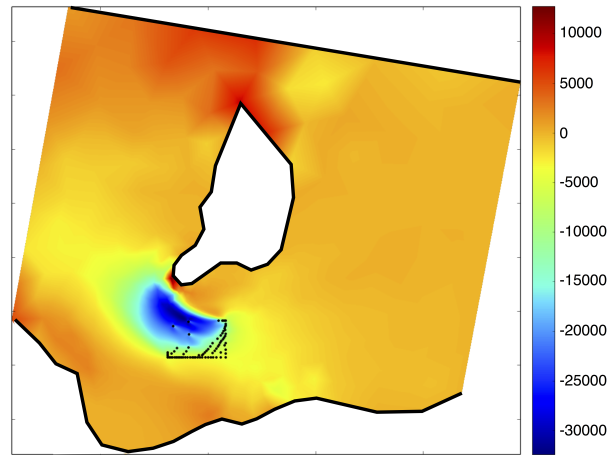


Fig. 12. Plot showing sensitivity of the power extracted from the flow with respect to the bottom friction. The colour bar shows dP/dc_b .

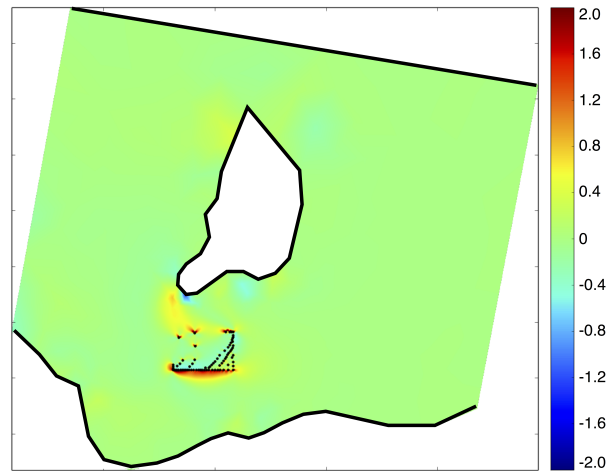


Fig. 13. Plot showing sensitivity of the power extracted from the flow with respect to the viscosity. The colour bar shows $dP/d\nu$.

flow would be able to infiltrate into the array from the side, increasing the power. Clearly the sensitivity is just a snapshot, and doesn't give the general trend of power with respect to viscosity. At a realistic viscosity many complex hydrodynamic structures would be forming and interacting within and outside the array. Adequately modelling such phenomena is a key focus for the authors and the *OpenTidalFarm* development team.

VII. CONCLUSIONS

In this paper a framework for the design of tidal turbine arrays (both size and micro-siting) has been presented, along with an approach for determining the sensitivity of the functional of interest with respect to the modelling input parameters. Optimising micro-siting and, by extension, array size is a computationally intensive task. The methodology presented here used techniques from statistical decision theory – such as surrogate modelling and variable fidelity sampling – to efficiently tackle this task by quickly finding the neigh-

bourhood of the optimal array size and focusing computational effort in that area; where it is most effective. This methodology was demonstrated on a semi-idealised case study based on the Inner Sound of the Pentland Firth, a site which is currently under development.

The Inner Sound site was modelled using the finite element method with a sinusoidal ebb / flood flow over a 12 hour period. It was found that, while the site could physically support several hundred turbines, the optimum number to maximise the financial return on the site was 80, arranged with barrages generally orientated perpendicular to the dominant flow pattern; a jet coming off the south of the island during the flood-flow phase. As noted in section VI-B3, more accurate turbine parametrisation is a key focus of continuing work. By capping the power (as a realistic power-curve would) one would expect profit to be maximised with fewer turbines. The difference in power extracted in the flood phase versus the ebb phase would also be reduced resulting in a more balanced, less flood-dominant orientation of the turbine barrages. Implementation of a realistic thrust curve would also affect the hydrodynamics – reducing wake lengths for turbine's in the most energetic parts of the channel, thereby facilitating a more closely packed micro-siting arrangement while still maximising the power.

Analysis of the sensitivity of the power produced by the optimum array showed that it could be strongly affected by incorrect assumptions of the depth and bottom friction to the north of the island – where it could redirect flow to the south, and where it might redirect the flood-phase jet more fully into the turbine area. Sensitivity analysis with respect to the viscosity implied that this may have a strong effect on the array design – especially with respect to turbines on the boundary of the turbine area. While this study was geared to being tractable on a desktop machine, future work is dedicated both to realistically capturing turbulent effects and using high performance computing to increase realism in other physical assumptions such as bathymetry, boundary positions and turbine parametrisation.

ACKNOWLEDGMENTS

The authors would like to acknowledge Imperial College London, the Engineering and Physical Sciences Research Council (projects: EP/J010065/1, EP/L000407/1 and EP/M011054/1) and a Center of Excellence grant from the Research Council of Norway to the Center for Biomedical Computing at Simula Research Laboratory for funding which supported this work.

REFERENCES

- [1] S. W. Funke, P. E. Farrell, and M. D. Piggott, “Tidal turbine array optimisation using the adjoint approach,” *Renewable Energy*, vol. 63, pp. 657 – 673, 2014.
- [2] T. Roc, D. C. Conley, and D. Greaves, “Methodology for tidal turbine representation in ocean circulation model,” *Renewable Energy*, vol. 51, pp. 448–464, 2013.
- [3] G. L. Barnett, S. W. Funke, and M. D. Piggott, “Hybrid global-local optimisation algorithms for the layout design of tidal turbine arrays,” *Submitted to Renewable Energy*, 2014.
- [4] T. A. Adcock, S. Draper, and T. Nishino, “Tidal power generation – a review of hydrodynamic modelling,” *Proceedings of the Institution of Mechanical Engineers, Part A: Journal of Power and Energy*, p. 0957650915570349, 2015.
- [5] D. M. Culley, S. W. Funke, S. C. Kramer, and M. D. Piggott, “Integration of cost modelling within the micro-siting design optimisation of tidal turbine arrays,” *Accepted. Renewable Energy*, 2015.
- [6] R. Vennell, “Tuning turbines in a tidal channel,” *Journal of Fluid Mechanics*, vol. 663, pp. 253 – 267, 2010.
- [7] R. Vennell, S. W. Funke, S. Draper, C. Stevens, and T. Divett, “Designing large arrays of tidal turbines: A synthesis and review,” *Renewable and Sustainable Energy Reviews*, vol. 41, pp. 454 – 472, 2015.
- [8] A. Logg, K. A. Mardal, and G. Wells, *Automated solution of differential equations by the finite element method: The FEniCS book*. Springer Science & Business Media, 2012, vol. 84.
- [9] C. Taylor and P. Hood, “A numerical solution of the Navier-Stokes equations using the finite element technique,” *Computers & Fluids*, vol. 1, no. 1, pp. 73–100, 1973.
- [10] P. E. Farrell, D. A. Ham, S. F. Funke, and M. E. Rognes, “Automated derivation of the adjoint of high-level transient finite element programs,” *SIAM Journal on Scientific Computing*, vol. 35, no. 4, pp. C369 – C393, 2013.
- [11] S. W. Funke and P. E. Farrell, “A framework for automated PDE-constrained optimisation,” *arXiv:1302.3894*, 2013.
- [12] A. Keane and P. Nair, *Computational approaches for aerospace design: The pursuit of excellence*. John Wiley & Sons, 2005.
- [13] S. N. Lophaven, H. B. Nielsen, and J. Søndergaard, “Dace-a matlab kriging toolbox, version 2.0,” Tech. Rep., 2002.
- [14] C. Rasmussen, “Gaussian processes for machine learning,” 2006.
- [15] M. S. Eldred, A. A. Giunta, S. S. Collis, N. A. Alexandrov, and R. M. Lewis, “Second-order corrections for surrogate-based optimization with model hierarchies,” in *Proceedings of the 10th AIAA/ISSMO Multidisciplinary Analysis and Optimization Conference, Albany, NY, Aug*, 2004.
- [16] T. A. Adcock, S. Draper, G. T. Housley, A. G. Borthwick, and S. Serhadlioğlu, “The available power from tidal stream turbines in the pentland firth,” *Proceedings of the Royal Society A: Mathematical, Physical and Engineering Science*, vol. 469, no. 2157, p. 20130072, 2013.